

Geology

Kamil Crater (Egypt): Ground truth for small-scale meteorite impacts on Earth

L. Folco, M. Di Martino, A. El Barkooky, M. D'Orazio, A. Lethy, S. Urbini, I. Nicolosi, M. Hafez, C. Cordier, M. van Ginneken, A. Zeoli, A.M. Radwan, S. El Khrepy, M. El Gabry, M. Gomaa, A.A. Barakat, R. Serra and M. El Sharkawi

Geology published online 5 January 2011;
doi: 10.1130/G31624.1

Email alerting services click www.gsapubs.org/cgi/alerts to receive free e-mail alerts when new articles cite this article

Subscribe click www.gsapubs.org/subscriptions/ to subscribe to *Geology*

Permission request click <http://www.geosociety.org/pubs/copyrt.htm#gsa> to contact GSA

Copyright not claimed on content prepared wholly by U.S. government employees within scope of their employment. Individual scientists are hereby granted permission, without fees or further requests to GSA, to use a single figure, a single table, and/or a brief paragraph of text in subsequent works and to make unlimited copies of items in GSA's journals for noncommercial use in classrooms to further education and science. This file may not be posted to any Web site, but authors may post the abstracts only of their articles on their own or their organization's Web site providing the posting includes a reference to the article's full citation. GSA provides this and other forums for the presentation of diverse opinions and positions by scientists worldwide, regardless of their race, citizenship, gender, religion, or political viewpoint. Opinions presented in this publication do not reflect official positions of the Society.

Notes

Advance online articles have been peer reviewed and accepted for publication but have not yet appeared in the paper journal (edited, typeset versions may be posted when available prior to final publication). Advance online articles are citable and establish publication priority; they are indexed by PubMed from initial publication. Citations to Advance online articles must include the digital object identifier (DOIs) and date of initial publication.

Kamil Crater (Egypt): Ground truth for small-scale meteorite impacts on Earth

L. Folco¹, M. Di Martino², A. El Barkooky³, M. D'Orazio^{4,5}, A. Lethy⁶, S. Urbini⁷, I. Nicolosi⁷, M. Hafez⁶, C. Cordier¹, M. van Ginneken¹, A. Zeoli¹, A.M. Radwan⁶, S. El Khrepy⁶, M. El Gabry⁶, M. Gomaa⁶, A.A. Barakat⁸, R. Serra⁹, and M. El Sharkawi³

¹Museo Nazionale dell'Antartide Università di Siena, Via Laterina 8, 53100 Siena, Italy

²Istituto Nazionale di Astrofisica, Osservatorio Astronomico di Torino, 10025 Pino Torinese, Italy

³Department of Geology, Faculty of Sciences, Cairo University, Giza, Egypt

⁴Dipartimento di Scienze della Terra, Università di Pisa, Via S. Maria 53, 56126 Pisa, Italy

⁵Istituto di Geoscienze e Georisorse, Consiglio Nazionale delle Ricerche, Via G. Moruzzi 1, 56124 Pisa, Italy

⁶National Research Institute of Astronomy and Geophysics, Helwan, Egypt

⁷Istituto Nazionale di Geofisica e Vulcanologia, Via di Vigna Murata 605, 00143 Rome, Italy

⁸Egyptian Mineral Resources Authority, 3 Salah Salem Road, Abassiya, Cairo, Egypt

⁹Dipartimento di Fisica, Università di Bologna, Via Irnerio 46, 40126 Bologna, Italy

ABSTRACT

Small impact craters (<300 m in diameter) are rare on Earth and mostly deeply eroded, so that knowledge of their formation mechanism and the hazard small impactors constitute to human populations is largely based on physical models. We report on the geophysical investigation of the Kamil Crater we recently discovered in southern Egypt. The Kamil Crater is a <5 k.y. old impact crater 45 m in diameter, with a pristine ejecta ray structure. Such well-preserved structures have been previously observed only on extraterrestrial rocky or icy planetary bodies. This crater feature, and the association with an iron meteorite impactor and shock metamorphism, provides a unique impression of aspects of small-scale hypervelocity impacts on the Earth's crust. Contrary to current models, ground data indicate that iron meteorites with masses of tens of tons may be able to penetrate the atmosphere without substantial fragmentation.

INTRODUCTION

Small meteorite impact craters with diameters of as much as a few hundred meters are common surface structures on solid planetary bodies in the solar system. Statistics predict that impact events producing small craters on Earth occur on decadal to secular time scales (Brown et al., 2002; Bland and Artemieva, 2006). However, small craters are rare on Earth (only 15 craters <300 m in diameter out of 176 craters to 300 km in diameter; Earth Impact Database, 2010), due to a combination of atmospheric destruction of small impactors and the relative ease with which smaller craters can be buried by post-impact sediments or destroyed by erosion (Grieve, 2001). The few identified so far have lost many of their primary features and only carry fragmentary information. As a consequence, knowledge of their formation mechanism, their effect on the environment, and the hazard small impactors pose to human populations are largely based on theoretical models and experimental analogs. Here we expand on our discovery report (Folco et al., 2010) of a rayed impact crater 45 m in diameter on a Cretaceous sedimentary target in the East Uweinat district (22°01'06"N, 26°05'15"E; Fig. 1), southern Egypt. It has been named Kamil Crater after the only named topographic feature in the region, the Gebel Kamil, ~65 km due east-northeast of the crater location.

The Kamil Crater was identified by V. De Michele (former curator of the Natural History Museum in Milan, Italy) during a Google Earth™ "low flight" (1000 m above ground level). QuickBird satellite images revealed a several decameter-sized crater (Fig. 1) in a rocky desert plain ~600 m above sea level, with a number of ejecta rays, highlighting the exceptional freshness of the structure (compare it with the only previously

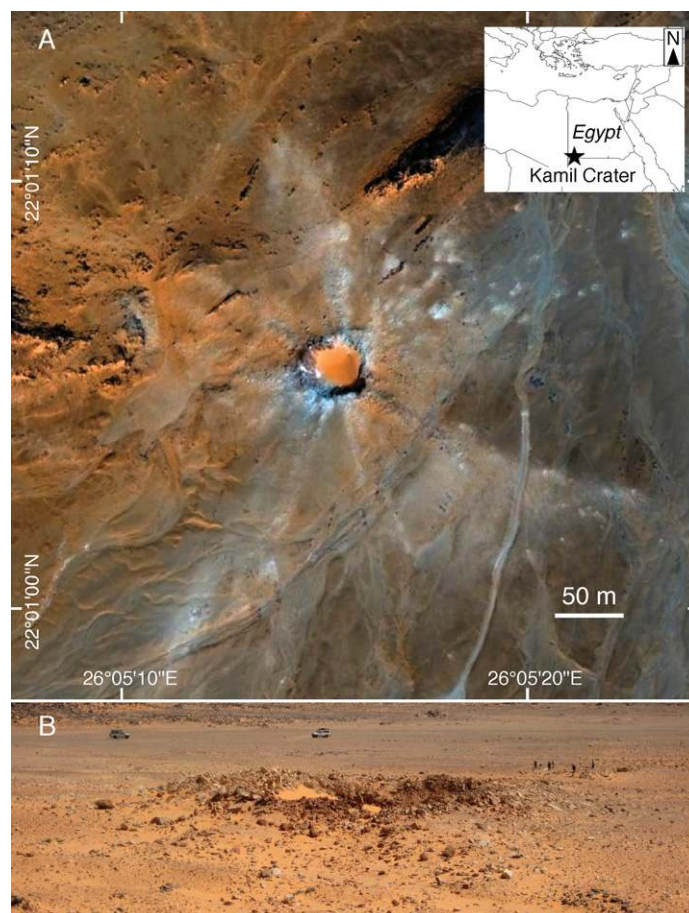


Figure 1. Kamil Crater, southern Egypt. A: Enhanced true color QuickBird satellite image (22 October 2005; courtesy of Telespazio); note simple crater structure and prominent ejecta ray pattern. Inset: location map. B: View of crater from west.

known rayed craters on Earth, craters 3 and 4 of the Henbury crater field, Australia; e.g., West et al., 2010). The thousands of iron meteorite specimens (Figs. 2A and 2B) found scattered within the crater and in the surrounding area during a preliminary survey in February 2009 confirmed the meteoritic impact origin of the crater. A geophysical expedition was then

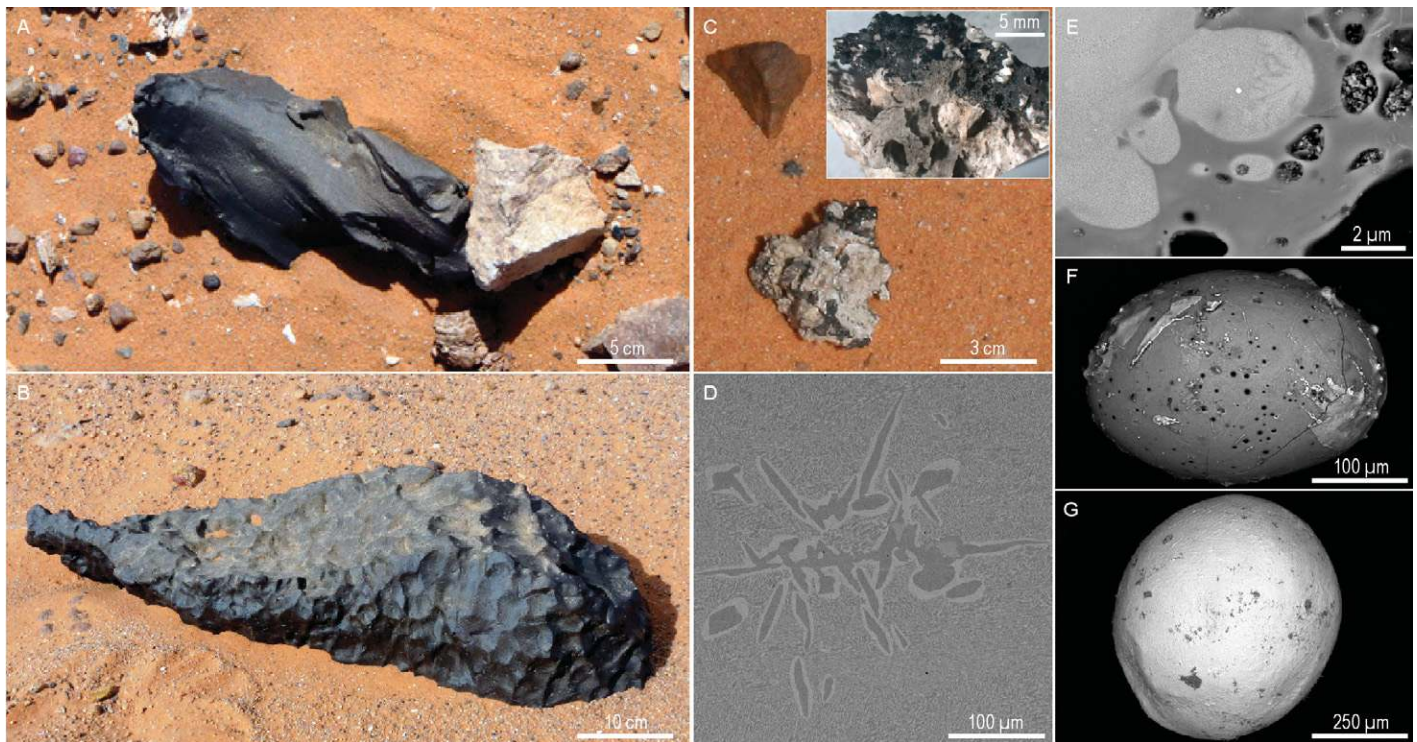


Figure 2. Field photographs and backscattered electron micrographs of iron meteorite, named Gebel Kamil, and impact glass associated with Kamil Crater. **A:** One of thousands of meteorite fragments (shrapnel) found scattered in crater and surrounding area. **B:** An 83 kg meteorite specimen found 230 m due north of crater showing regmaglypts. **C:** Pumiceous impact glass found scattered in ejecta blanket. Note siliceous (white) and Fe-Ni-rich (dark) glasses deriving from melting of target and projectile (inset). **D:** Microscopic kamacite spindles in plesitic groundmass observed in one sectioned shrapnel characteristic of ataxite iron meteorites. **E:** Textural relationships between siliceous (dark) and Fe-Ni-rich (bright) impact glasses. **F:** Microscopic spheroid of impact glass found in magnetic fraction <5 mm of ejecta blanket. **G:** Molten droplet of impactor from same magnetic fraction consisting of Fe-Ni oxides.

carried out (see the GSA Data Repository¹) in February 2010 in order to describe this model impact structure and contribute to our understanding of small-scale meteorite impacts on Earth.

CRATER

The Kamil Crater occurs on exposed pale sandstones (mainly quartz arenites) of the Gifl Kebir Formation (Early Cretaceous) that are locally overlain by a few centimeters of soil (Fig. 1; Fig. DR1 in the Data Repository). The sandstones have subhorizontal bedding and constitute part of the sedimentary cover unconformably overlying the Precambrian crystalline basement (Klitzsch et al., 1987). High-precision topography obtained by a differential global positioning system survey reveals that the crater is circular with an average rim-crest diameter of 45 m (Fig. 3A). The crater is bowl shaped and has an upraised rim ~3 m above the presumed pre-impact surface (Fig. 3B), in accordance with expectations for simple crater structures (Melosh, 1989). Part of the northern wall of the crater is covered by a meter-thick eolian sand deposit. The ground-penetrating radar survey reveals that the true crater floor is at an average depth of 16 m below rim crest and that it is overlain by an ~6-m-thick crater-fill material consisting of displaced blocks and stratified fallout debris (Fig. 3B). The true crater floor gently slopes toward the southeast, suggesting a deeper excavation in this direction. At crater walls, bedding in the bedrock is upturned (up

to 40°) and dips radially outward. An overturned flap of ejected material is locally present at the rim crest. The diameter of the crater, the depth of the true crater floor, and the rim height agree with those predicted by cratering models (Collins et al., 2005) for a transient crater generated by an iron meteorite ~1.3 m in diameter (equivalent to 9.1×10^3 kg) impacting at a velocity of ~3.5 km s⁻¹, assuming an average meteoroid entry velocity of 18 km s⁻¹ and entry angle of 45° (note that, by decreasing the incident angle to 30°, similar morphometric parameters are obtained with impactor masses as much as two times larger). Centimeter-scale masses of pumiceous, siliceous glass derived from the impact melting of the target occur in and close to the crater (Figs. 2C and 2E), and indicate local attainment of shock pressures >60 GPa (e.g., Melosh, 1989). Some of these masses are associated with an Fe-Ni-rich dark glass, testifying to some melting of the projectile during impact.

The bulk of the debris ejected from the impact crater consists of sandstone fragments ranging from large boulders with masses to 4 t, to dust. Their pale color sharply contrasts with the darker color of the weathered bedrock, allowing easy detection both in the field and in satellite images (Fig. 1A). An ejecta blanket extends radially for ~50 m from the crater rim in a northward, eastward, and southward direction. The three longest ejecta rays are straight and extend for as much as 350 m from the crater rim and trend to the north, southeast, and southwest. A triangular zone almost free of ejecta (i.e., forbidden zone) occurs on the western side of the crater. This asymmetric distribution of ejecta suggests that the Kamil Crater formed by a moderately oblique (i.e., 30°–45°) impact (Melosh, 1989), likely from the northwestern quadrant. This is consistent with the asymmetry of the slope of the true crater floor (Fig. 3B). Note that according to models (Gault and Wedekind, 1978; Schultz et al., 2009),

¹GSA Data Repository item 2011074, Table DR1, methods and mineral chemistry data, Figures DR1 and DR2 (field photos of the Kamil Crater and associated structures), and Figure DR3 (micrographs of the associated meteorite, Gebel Kamil), is available online at www.geosociety.org/pubs/ft2011.htm, or on request from editing@geosociety.org or Documents Secretary, GSA, P.O. Box 9140, Boulder, CO 80301, USA.

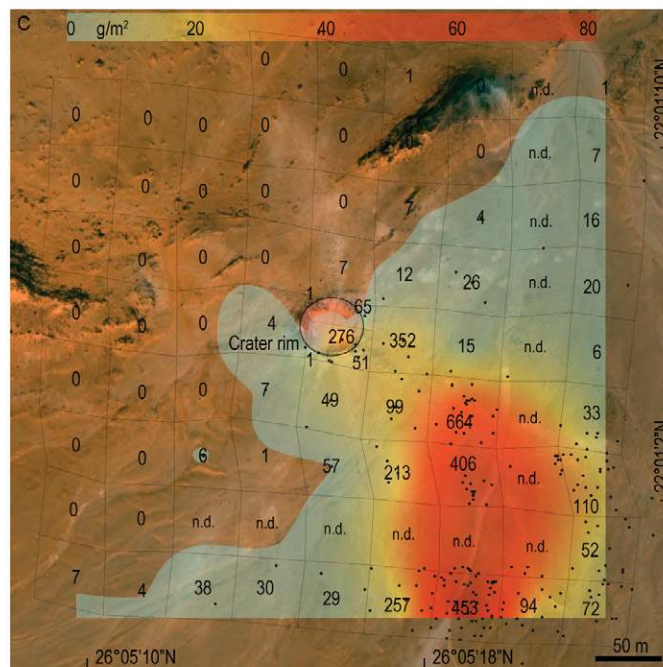
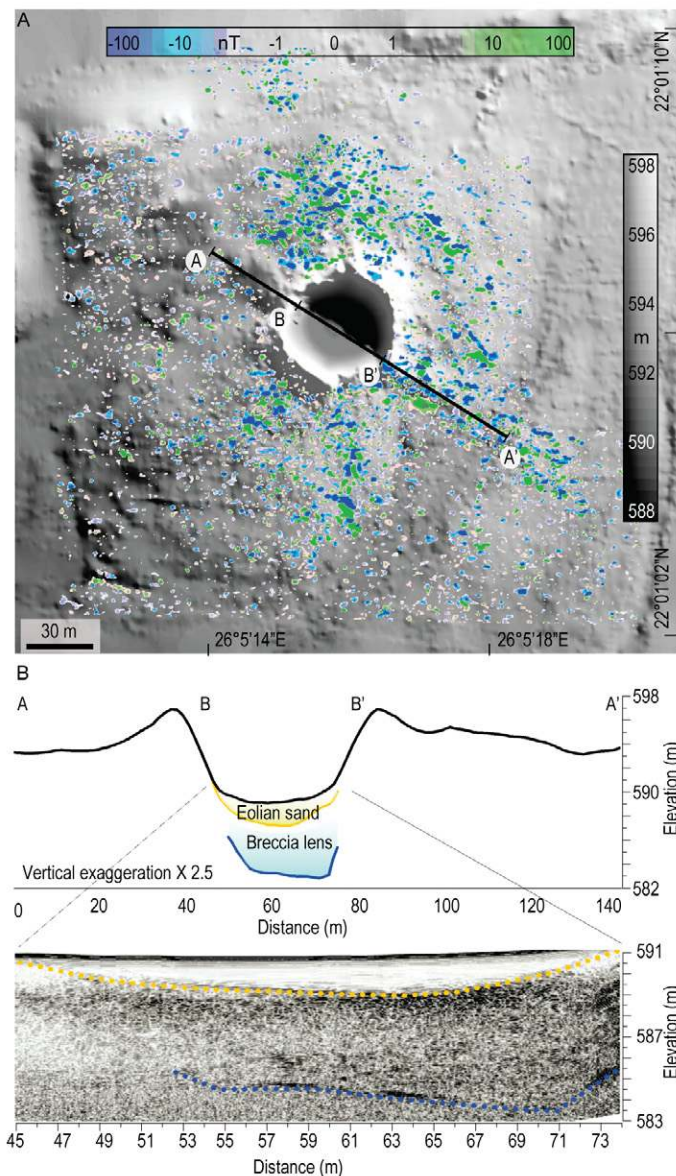


Figure 3. Selected geophysical data from Kamil Crater. A: Digital elevation model (DEM; plus shaded relief) with superimposed magnetic anomaly map detected after systematic searches and collection of meteorites >10 g. Maxima are localized along northern, southeastern, and southwestern ejecta rays, where abundant microscopic melt particles of projectile are interspersed within ejecta blanket. B: Representative section across crater (upper panel; see A for section line) based on DEM and ground-penetrating radar survey of crater floor (lower panel) and featuring some of main morphometric parameters described in text. C: Schematic representation of meteorite distribution obtained from systematic searches within 50 × 50 m cells of 450 × 450 m area centered at crater. Numbers of collected specimens are reported at each cell center (n.d. = not determined). Gray dots represent specimens >500 g. Meteorite concentration to southeast defines downrange jet of impactor debris produced by oblique impact from northwestern quadrant.

low incident angles (<30°) produce elliptical craters with steeper uprange crater walls, as well as cardioid or arachnoid patterns of the ejecta.

A prehistoric trail ~100 m due north of the crater is overlain by rock sandstone ejected from the crater (Fig. DR2). Although many artifacts were found in the ruins of prehistoric settlements a few hundred meters due east and south of the crater, there was no evidence of tools made from the iron meteorite. The human occupation of this region ended in the middle Holocene, ~5 k.y. ago, with the onset of hyperarid conditions (Kuper and Kröpelin, 2006). We therefore conclude that the impact occurred within the past 5000 yr, in agreement with the freshness of the impact structure and meteorite preservation (see following). The Kamil crater is visible in the 1972 Landsat satellite images, providing a minimum age limit for the impact event.

METEORITE

A systematic search for meteorites was conducted within a 450 m × 450 m area around the crater and along a number of concentric and radial traverses as much as 1.7 km from the crater. Approximately 50% of the meteorite-bearing surface was covered; 5178 meteorite specimens totaling ~1.71 t were identified. All specimens are shrapnel up to 34 kg in mass,

i.e., fragments produced by the explosion of the impactor upon hypervelocity collision with the target (Fig. 2A). The only exception is an 83 kg specimen completely covered with well-developed regmaglypts (Fig. 2B) found 230 m due north of the crater. This indicates that the Kamil Crater was generated by an impactor that landed nearly intact without significant fragmentation in the atmosphere. Shrapnel is concentrated in terms of mass and number to the southeast, whereas it is virtually absent in the northwestern quadrant (Fig. 3C). This asymmetric distribution defines the downrange jet of impactor debris produced by an oblique impact from the northwestern quadrant, and a decoupling with bedrock ejecta. Shrapnel as heavy as ~400 g was found 1.6 km due east-southeast of the crater, demonstrating the force related to the formation of this explosive jet.

Meteorites were typically found in desert soil (Figs. 2A and 2B) or on exposed bedrocks. They have a fresh appearance, except for some iron oxyhydroxide occurring on surfaces immersed in soil. The exposed surfaces of shrapnel are dark brown (Fig. 2A) and finely pitted due to the action of wind-driven sand. Shrapnel shows shapes varying from flattened, sharp-edged and jagged to more rounded, smooth, and equidimensional. Twisted edges are very common. The individual with regmaglypts (Fig. 2B) preserves patches of fusion crust, indicating a

short terrestrial residence time. Etched sections display an ataxitic texture speckled by millimeter-sized assemblages of schreibersite, troilite, and daubréelite crystals surrounded by swathing kamacite (Fig. DR3; Table DR1). Scanning electron microscopy reveals the occurrence of aligned clusters of kamacite spindles ($20 \pm 5 \mu\text{m}$ wide) rimmed by taenite (Fig. 2D), set in a matrix of duplex plessite consisting of kamacite and taenite lamellae ($1\text{--}5 \mu\text{m}$ in thickness) arranged in a micro-Widmanstätten pattern. Common shear dislocations in the sectioned shrapnel record the high stress associated with the impact. The composition of the metal, determined by inductively coupled plasma–mass spectrometry (D’Orazio and Folco, 2003), is Co = 0.75 wt%, Ni = 19.8 wt%, and Cu = 464, Ga = 49, Ge = 121, As = 15.6, Mo = 9.1, Ru = 2.11, Rh = 0.75, Pd = 4.8, Sn = 2.49, Sb = 0.26, W = 0.66, Re = 0.04, Ir = 0.39, Pt = 3.5, Au = 1.57 (all in $\mu\text{g g}^{-1}$). The Kamil meteorite, named Gebel Kamil, is classified as an ungrouped Ni-rich ataxite.

After collecting meteorites >10 g, a geomagnetic survey was carried out in an $\sim 250 \times 250 \text{ m}$ area with the crater at its center. Magnetic anomaly data show no evidence of buried meteorites larger than some tens of centimeters in size. Detected anomalies (Fig. 3A) are associated with the ejecta blanket, with maxima localized along the northern, southeastern, and southwestern ejecta rays (Fig. 3A). The <5 mm magnetic extracts of the ejecta blanket from these sites, containing abundant microscopic particles of Fe–Ni-rich silicate glass (up to a few tens of g m^{-2}) and microscopic spherules consisting of Fe–Ni oxides (Figs. 2F and 2G), provide a likely explanation for the magnetic anomalies.

DISCUSSION

The Kamil Crater provides tangible evidence of the geological effects generated by the impact of meter-sized iron meteorites on Earth’s crust. Due to the high degree of preservation, the Kamil Crater allows definition of all of the characteristics of small-scale meteoritic impacts, including the rayed structure, shock metamorphism, and preservation of the impactor in the form of meteorites. This unique, internally consistent data set will be critical in calibrating small-scale impact cratering models. In particular, on the basis of meteorite and Fe–Ni-rich microscopic particle distribution, we estimate that the total mass of the impactor is $\sim 5\text{--}10 \times 10^3 \text{ kg}$ (see the Data Repository), corresponding to a pre-atmospheric mass of $\sim 20\text{--}40 \times 10^3 \text{ kg}$ (Bland and Artemieva, 2006). According to models (Bland and Artemieva, 2003), iron masses $< 3 \times 10^6 \text{ kg}$ normally fragment upon impact with Earth’s atmosphere, thereby reducing significantly the energy of the impact at Earth’s surface. This model result found support from a study of small terrestrial craters that showed that 9 of the 12 impacts resulting from iron meteorites in the above mass range produced multiple craters (Bland and Artemieva, 2006). The current statistics, which include the recently discovered Whitecourt Crater (Herd et al., 2008) and the Kamil Crater, indicate, however, that $\sim 35\%$ of the iron meteorites in the above mass range are not substantially fragmented in the atmosphere. We suggest that theoretical calculations that take into account variable mechanical properties of iron meteorites associated with their variable textures (e.g., ataxites versus octahedrites; Furnish et al., 1995) may produce more accurate models for meteorite-atmosphere interaction, impact cratering, and hazard assessment.

The Gebel Kamil is the first large iron meteorite from Egypt. The <5000 yr age of this major fall poses the question of a possible link with the “iron of heaven” recurring in the Egyptian hieroglyphic records (through the XIXth Dynasty, ca. 1298–1187 B.C.; e.g., Bell and Alpher, 1969).

ACKNOWLEDGMENTS

Work was carried out within the framework of the “2009 Italian–Egyptian Year of Science and Technology.” We thank T. Hussein (President of the Egyptian National Academy of Science and Technology) and F. Porcelli (Scientific Attaché, Italian Embassy, Egypt) for diplomatic support; the Egyptian Army for logistical support; F. Speranza and P. Rochette for helpful discussion during the planning of the geophysical campaign; the European Commission (through the Marie Curie Actions—Research Training Networks ORIGINS project), the Fondazione Cassa di Risparmio di Torino, the Banca Monte dei Paschi di Siena S.p.A., and Telespazio S.p.A. (in the framework of the European Space Agency Space Situational Awareness program) for financial support.

REFERENCES CITED

- Bell, L., and Alpher, B., 1969, The Egyptian Hieroglyphic Group: Meteoritics, v. 3, p. I–II.
- Bland, P.A., and Artemieva, N.A., 2003, Efficient disruption of small asteroids by Earth’s atmosphere: *Nature*, v. 424, p. 288–291, doi: 10.1038/nature01757.
- Bland, P.A., and Artemieva, N.A., 2006, The rate of small impacts on Earth: *Meteoritics & Planetary Science*, v. 41, p. 607–631, doi: 10.1111/j.1945-5100.2006.tb00485.x.
- Brown, P.A., Spalding, R.E., ReVelle, D.O., Tagliaferri, E., and Worden, S.P., 2002, The flux of small near-Earth objects colliding with the Earth: *Nature*, v. 420, p. 294–296, doi: 10.1038/nature01238.
- Collins, G.S., Melosh, H.J., and Marcus, R.A., 2005, Earth impact effects program: A web-based computer program for calculating the regional and environmental consequences of a meteoroid impact on Earth: *Meteoritics & Planetary Science*, v. 40, p. 817–840, doi: 10.1111/j.1945-5100.2005.tb00157.x.
- D’Orazio, M., and Folco, L., 2003, Chemical analysis of iron meteorites by inductively coupled plasma–mass spectrometry: *Geostandards Newsletter*, v. 27, p. 215–225, doi: 10.1111/j.1751-908X.2003.tb00723.x.
- Earth Impact Database, 2010, The Earth Impact Database: Planetary and Space Science Centre, University of New Brunswick, Canada, <http://www.passc.net/EarthImpactDatabase>.
- Folco, L., and 17 others, 2010, The Kamil Crater in Egypt: *Science*, v. 329, p. 804, doi: 10.1126/science.1190990.
- Furnish, M.D., Boslough, M.B., Gray, G.T., and Remo, J.L., 1995, Dynamical properties measurements for asteroid, comet and meteorite material applicable to impact modeling and mitigation calculations: *International Journal of Impact Engineering*, v. 17, p. 341–352, doi: 10.1016/0734-743X(95)99860-T.
- Gault, D.E., and Wedekind, J.A., 1978, Experimental studies of oblique impact: *Proceedings of the Ninth Lunar and Planetary Science Conference*, p. 3843–3875.
- Grieve, R.A.F., 2001, The terrestrial cratering record, *in* Peucker-Ehrenbrink, B., and Schmitz, B., eds., *Accretion of extraterrestrial matter through Earth’s history*: New York, Springer-Verlag, p. 379–402.
- Herd, C.D.K., Froese, D.G., Walton, E.L., Kofman, R.S., Herd, E.P.K., and Duka, M.J.M., 2008, Anatomy of a young impact event in central Alberta, Canada: Prospects for the missing Holocene impact record: *Geology*, v. 36, p. 955–958, doi: 10.1130/G25236A.1.
- Klitzsch, E., List, F.K., and Pöhlmann, G., 1987, Geological map of Egypt, Gilf Kebir Plateau: Egyptian General Petroleum Corporation/Conoco, 1 sheet, scale 1:500 000.
- Kuper, R., and Kröpelin, S., 2006, Climate-controlled Holocene occupation in the Sahara: Motor of Africa’s evolution: *Science*, v. 313, p. 803–807, doi: 10.1126/science.1130989.
- Melosh, H.J., 1989, *Impact cratering: A geologic process*: Oxford Monographs on Geology and Geophysics 11: Oxford, Oxford University Press, 245 p.
- Schultz, P.H., Anderson, J.B.L., and Hermalyn, B., 2009, Origin and significance of uprange ray patterns: Lunar and Planetary Institute, 40th Lunar and Planetary Science Conference Proceedings, abs. 2496 (CD-ROM).
- West, M.D., Clarke, J.D.A., Thomas, M., Pain, C.F., and Walter, M.R., 2010, The geology of Australian Mars analogue sites: *Planetary and Space Science*, v. 58, p. 447–458, doi: 10.1016/j.pss.2009.06.012.

Manuscript received 30 July 2010

Revised manuscript received 30 September 2010

Manuscript accepted 4 October 2010

Printed in USA